Calculation and Analysis of Water Environmental Capacity of Typical Rivers in the Loess Area of Northern Shaanxi Based on a One-Dimensional Water Quality Model

Qian Huang[1,*], Pu Zhang[1], Yuan Zhang[1], Xiaohu Du[2], Chunxing Guan[1], Xiaokun Xu[1], Lu Zhang[1], Bo Yang[1]
[1]Shaanxi Modern Architectural Design and Research Institute Co., Ltd., Xi'an, Shaanxi, China
[2]Huoqi County Water Resources Bureau, Lu'an, Anhui, China
**Corresponding Author*

Abstract: Water environmental capacity (WEC) is a key indicator for pollutant load control and watershed management. Taking the Xingzi, Xichuan, and Pingqiaochuan rivers in Ansai District, Yan'an City as case studies, this study selected COD, NH_3-N, and TP as control indicators and applied a one-dimensional water quality model based on GB/T 25173–2010 to estimate WEC under wet (10%), normal (50%), and dry (90%) hydrological years. Results showed that all three rivers maintained surplus WEC and generally good water quality. WEC followed the pattern of wet year > normal year > dry year and was significantly higher in summer than in winter. Among the rivers, Xichuan River had the largest WEC, followed by Xingzi River, while Pingqiaochuan River had the smallest. It is recommended that dry-year WEC be adopted as the baseline for total pollutant load control, with strengthened management of rural non-point source pollution and improved dry-season monitoring and early-warning systems. This study provides scientific support for regional water environmental management and pollutant control.

Keywords: Water Environmental Capacity; Water Quality Model; Design Hydrological Conditions; Non-Point Source Pollution; Loess Plateau

1. Introduction

The pollution load capacity of a river refers to the maximum amount of pollutants that a water body can accommodate under specific hydrological conditions, water quality objectives, pollutant migration and transformation mechanisms, and design hydrological scenarios. It serves as a crucial scientific basis for implementing total pollution control and watershed water environment management [1,2]. With the deepening implementation of China's "Action Plan for Water Pollution Prevention and Control" ("Water Ten Measures"), there is an increasing demand for precise calculation of river pollution load capacity across regions, particularly in ecologically fragile and water-scarce areas such as the Loess Plateau, where scientifically determining pollution load capacity has become a key step in safeguarding regional aquatic ecological security [3,4].

Ansai District in Yan'an City lies in the middle reaches of the Yellow River and the upper reaches of the Yan River, representing a typical loess hilly-gully region characterized by severe soil erosion and highly uneven spatiotemporal distribution of water resources. In recent years, accelerated urbanization and intensified agricultural activities have led to growing concerns over non-point source pollution—including rural domestic wastewater, agricultural fertilizer runoff, and livestock emissions—posing significant threats to river water quality [5]. Xingzi River, Xichuan River, and Pingqiao River are major tributaries of the Yan River; their water quality not only affects local drinking water safety and agricultural irrigation but also exerts cascading impacts on downstream Yan'an city and the Yellow River. However, systematic assessments of pollution load capacity for these three small-to-medium rivers remain lacking, resulting in insufficient quantitative benchmarks for water environmental management.

Research on water environmental capacity originated in developed countries such as the United States and Japan during the 1960s, primarily applied to water quality management in the Great Lakes and the Mississippi River Basin

[6]. China introduced the concept of water environmental capacity in the late 1970s and has since conducted extensive applications in major rivers and lakes including the Yangtze, Yellow, Huai, and Taihu Rivers [7,8]. Regarding computational methods, zero-dimensional models are suitable for lakes or small water bodies, one-dimensional models for medium-to-small rivers, and two-dimensional models for large, wide, shallow rivers or estuarine zones [9-11]. Most studies in the Loess Plateau region have focused on larger rivers such as the Wei River and Yan River [12,13], while systematic calculations for smaller tributaries (e.g., Pingqiao River) remain limited. Moreover, few studies have simultaneously considered variations in pollution load capacity across different hydrological years (wet, normal, and dry).

This study focuses on Xingzi River, Xichuan River, and Pingqiao River, aiming to achieve the following: (1) establish a pollution load capacity calculation framework applicable to small-to-medium loess rivers; (2) calculate the COD, ammonia nitrogen, and TP pollution load capacities of the three rivers under wet, normal, and dry hydrological conditions; (3) analyze the spatiotemporal variation characteristics and key influencing factors of pollution load capacity; and (4) provide targeted recommendations for water environmental management. The innovation lies in comprehensively covering both main streams and tributaries, distinguishing multiple river segments and hydrological years, and integrating simplified non-point source modeling methods, thereby filling the gap in systematic research on pollution load capacity for small-to-medium rivers in this region.

2. Materials and Methods

2.1 General Natural Geography

Ansai District is located in the northern part of Shaanxi Province and the northwestern part of Yan'an City, with geographical coordinates ranging from 108°45′ to 109°31′ east longitude and 36°31′ to 37°20′ north latitude, covering a total area of approximately 2,950 km². The terrain is dominated by loess ridges, mounds, and gullies, with elevations between 1,000 and 1,500 meters. The region has a warm temperate semi-arid continental climate, with an average annual temperature of 8.8°C and an average annual precipitation of about 500 mm, most of which occurs from July to September—accounting for over 60% of the annual rainfall—and high evaporation rates. The Xingzi River, Xichuan River, and Pingqiao River are all first-order tributaries of the Yan River, flowing into it from northwest to southeast. The basic hydrological characteristics of these three rivers are shown in Table 1.

Table 1. Basic Hydrological Characteristics of Rivers

River	Total length (km)	Length within Ansai district (km)	Drainage area (km²)	Average annual runoff ($10^4 m^3$)	Average gradient (‰)	Average long-term flow rate (m³/s)
Xingzi	102.8	40.0	1486.1	2300	6.2	0.73
Xichuan	65.3	42.5	809.0	2900	7.8	0.92
Pingqiao	39.3	39.3	337.8	620	9.3	0.20

2.2 Current Water Environment Quality

Based on on-site sampling (Figure 1) and testing (with three sections each at the upstream, middle, and downstream of each river), the water quality of the three rivers all met the Class III standards of the "Surface Water Environmental Quality Standards" (GB 3838-2002) (COD ≤ 20 mg/L, ammonia nitrogen ≤ 1 mg/L, TP ≤ 0.2 mg/L), but showed an upward trend along the river course. The COD in the downstream of Xiesi River reached 18.5 mg/L, approaching the limit; the water quality in the upstream of Xichuan River was the best (COD 6.2 mg/L); the TP concentration in the middle and downstream of Pingqiao River (0.12 - 0.15 mg/L) was relatively high, possibly related to the discharge from livestock and poultry farming. The background water quality values are shown in Table 2.

Figure 1. On-Site Sampling Diagram

Table 2. River Water Quality Test Results (Unit: mg/L)

River	Section locations	COD	NH_3-N	TP
Xingzi	Upstream (Wang Yao)	16.4	0.11	0.02

	Middle (Zha'an Town)	17.7	0.20	0.04
	Downstream (Yanhe Bay)	18.5	0.27	0.06
Xichuan	Upstream (Du Jia River)	6.2	0.04	0.11
	Middle (Tujiaowan)	10.1	0.07	0.14
	Downstream (Xichuankou)	12.3	0.19	0.18
Pingqiao	Upstream (Source)	8.4	0.08	0.04
	Middle (Pingqiao Town)	16.4	0.11	0.12
	Downstream (Jianhua)	18.8	0.17	0.15

2.3 Composition of Pollution Sources

There are no industrial point source discharge outlets in the study area. All pollution sources are non-point sources. Based on the "Shaanxi Statistical Yearbook", "Yanchang Statistical Yearbook", and the livestock breeding pollution coefficient (GB18596-2001), the total pollutant emissions in the study area in 2022 were: COD 1395.96 t, ammonia nitrogen 144.92 t, and TP 26.68 t. Among them, rural domestic pollution sources accounted for 43.93% of COD and 45.85% of ammonia nitrogen, being the largest contributing source; livestock breeding accounted for 31.06% of TP, being the main phosphorus source. The composition of pollution sources is shown in Table 3.

Table 3. Summary of Pollutant Sources in the Watershed (Unit: t)

Pollution source	COD	Percentage (%)	NH_3-N	Percentage (%)	TP	Percentage (%)
Rural life	868.75	43.93	101.35	45.85	8.69	22.56
Agricultural production	94.94	4.80	14.24	6.44	6.03	15.66
Livestock and poultry	432.27	21.86	29.33	13.27	11.96	31.06
Total	1395.96	100	144.92	100	26.68	100

2.4 Research Methods

2.4.1 Pollutant absorption capacity calculation

According to the "Calculation Procedure for Water Pollution Capacity of Water Bodies" (GB/T 25173-2010), for medium and small-sized river sections with an average annual flow rate Q less than 150 m³/s, the pollutants can be considered to be uniformly mixed in the cross-section, and a one-dimensional water quality model is selected. The variation law of pollutant concentration along the river section is (Equation 1):

$$C_x = C_0 \exp\left(-K\frac{x}{u}\right) \quad (1)$$

C_x is the pollutant concentration after flowing x distance, *mg/L*; C_0 is the initial cross-sectional pollutant concentration, *mg/L*; x is the distance along the longitudinal river section, m; u is the average flow velocity of the cross-section, m/s; K is the attenuation coefficient of the pollutant, *1/s*.

The water pollution capacity of the water body is calculated according to Equation 2:

$$M = (C_s - C_{x=L})(Q_0 + Q_p) \quad (2)$$

M is the water pollution capacity of the water body, *g/s*; C_s is the target water quality concentration value, mg/L; Q_0 is the flow rate of the initial cross-section, *m³/s*; Q_p is the wastewater discharge flow rate, *m³/s*; $C_{x=L}$ is the cross-sectional pollutant concentration in the water function area, *mg/L*.

Since there are no point sources in the study area, non-point sources are approximated as uniformly input in the middle of the river section. At this time, the concentration of the lower cross-section is calculated according to Equation 3, and then substituted into Equation 2 to calculate the pollution capacity.

$$C_{x=L} = C_0 \exp\left(-K\frac{L}{u}\right) + \frac{m}{Q_0}\exp\left(-K\frac{L}{u}\right) \quad (3)$$

m is the pollutant inflow rate into the river, *g/s*; the rest are the same as the formulas above.

2.4.2 Determination of design hydrological conditions

According to the requirements of the procedure, the 90% guarantee rate lowest monthly average flow rate is used as the design flow rate. For Xingzi River, based on the long series data of the hydrological station of Wangyao Reservoir (1980-2020), the Xichuan River and Pingqiao River are estimated using the area analogy method (Equation 4) [14]:

$$Q_2 = Q_1(P_2/P_1)(A_2/A_1)(1-\lambda) \quad (4)$$

Q_1 and Q_2 are the runoff volumes of the two river basins; P_1 and P_2 are the precipitation amounts of the two river basins; A_1 and A_2 are the areas of the two river basins; λ is the difference coefficient of water and soil conservation measures of the two river basins, with a range of 0 to 1.

This work uses the 90% guarantee rate lowest monthly average flow rate as the design flow rate, and calculates the 10%, 50%, and 90% guarantee rate (flood year, normal year, and dry year) monthly average flows of the three rivers using the empirical frequency curve distribution. Different design flow conditions are shown in Table 4.

Table 4. Design Flow Conditions (Unit: m^3/s)

Xingzi River design flow rate			
Month	10%	50%	90%
1	0.35	0.84	0.66
2	0.59	1.67	0.54
3	2.06	1.56	0.61
4	1.40	0.68	0.86
5	0.84	0.73	0.56
6	0.59	2.48	0.56
7	12.07	4.35	1.65
8	12.09	2.33	2.84
9	1.90	2.07	0.62
10	1.29	3.79	2.13
11	1.04	0.99	0.82
12	0.97	0.61	0.74
Xichuan River design flow rate			
Month	10%	50%	90%
1	0.19	0.46	0.36
2	0.32	0.91	0.29
3	1.12	0.85	0.33
4	0.76	0.37	0.47
5	0.46	0.40	0.30
6	0.32	1.35	0.30
7	6.57	2.37	0.90
8	6.58	1.27	1.55
9	1.04	1.13	0.34
10	0.70	2.06	1.16
11	0.57	0.54	0.44
12	0.53	0.33	0.41
Pingqiao River design flow rate			
Month	10%	50%	90%
1	0.08	0.19	0.15
2	0.13	0.37	0.12
3	0.46	0.35	0.14
4	0.31	0.15	0.19
5	0.19	0.16	0.12
6	0.13	0.55	0.12
7	2.68	0.97	0.37
8	2.68	0.52	0.63
9	0.42	0.46	0.14
10	0.29	0.84	0.47
11	0.23	0.22	0.18
12	0.22	0.14	0.17

2.4.3 Parameter determination and sensitivity analysis

(1) Degradation coefficient

The degradation coefficient K is determined using the measured section back-calculation method and combined with regional literature analogy. The formula is (Equation 5):

$$K = (LnC_1 - LnC_2)/d \quad (5)$$

The degradation coefficient of *K pollutants, 1/d;* C_1 is the pollutant concentration at the upstream section, *mg/L*; C_2 is the pollutant concentration at the downstream section, *mg/L*; *d* is the distance between the upstream and downstream sections, *km*.

Based on the measured concentration differences between the upstream and downstream and the section spacing, the K value of COD was calculated to be 0.20-0.25 d^{-1}, ammonia nitrogen 0.12-0.18 d^{-1}, and TP 0.10-0.14 d^{-1}. Considering the hydraulic conditions, water temperature (annual average 10-15°C) and the sediment adsorption effect in the loess region, the final values were: COD: 0.20 d^{-1}, ammonia nitrogen: 0.15 d^{-1}, TP: 0.12 d^{-1}.

(2) Flow velocity and hydraulic radius

The water level-flow relationship was calculated using the Manning formula (Equation 6):

$$V = \frac{k}{n} R_h^{2/3} \cdot S^{1/2} \quad (6)$$

V represents velocity; K is the conversion constant, with an international unit value of 1; n represents the roughness coefficient, which is a coefficient that comprehensively reflects the influence of the roughness of the pipe and channel walls on the flow; its value is generally measured from experimental data and can be selected from a table when used; Rh is the hydraulic radius, which is the ratio of the fluid cross-sectional area to the wet perimeter; S is the slope.

Based on the measured data of the large cross-section, the roughness coefficient n is set at 0.035 to 0.045 (for gravel and weeds), the hydraulic radius R is 0.2 to 0.8 m, and the river slope S is 0.006 to 0.009. The calculated flow velocity range is 0.2 to 0.8 m/s, which is in good agreement with the measured values (error < 15%).

(3) Sensitivity analysis

The perturbation analysis method (parameters ±20%) is used to investigate the sensitivity of K, C_0, and u to the pollutant carrying capacity. Taking the dry season of Xingzi River as an example, the results show that: a ±20% change in the K value causes a ±18% to ±22% change in the pollutant carrying capacity; a ±20% change in C_0 causes a ±6% to ±10% change in the pollutant carrying capacity; a ±20% change in u causes a ±12% to ±15% change in the pollutant carrying capacity. This indicates that the K value is the most sensitive, followed by the flow velocity, and the background concentration has a relatively smaller influence. Therefore, in practical applications, the K value should be prioritized for calibration.

3. Results and Analysis

3.1 Different Water Pollution Capacity in Different Hydrological Years

Table 5. Water Pollution Capacity in Different Hydrological Years (units: t/a)

River	Hydrological	COD	NH_3-N	TP
Xingzi	10%	873.63	168.50	32.23
	50%	548.73	105.84	20.25
	90%	312.18	60.21	11.52
Xichuan	10%	1737.48	136.40	9.01
	50%	1073.14	83.70	5.29
	90%	589.44	45.33	2.58
Pingqiao	10%	513.59	37.37	6.52
	50%	310.54	22.77	3.96
	90%	169.09	12.14	2.10

The annual water pollution capacity of the three rivers under the guarantee rate in flood years, normal years, and dry years is shown in Table 5. The water pollution capacity of the three rivers in each hydrological year is all positive. The current pollution load (COD 1395.96 t/a, ammonia nitrogen 144.92 t/a, TP 26.68 t/a) has not exceeded the water pollution capacity in the dry year, indicating that the water quality is up to standard and there is a certain safety margin. The water pollution capacity significantly increases with the increase of runoff: the COD pollution capacity in flood years is approximately 2.8 to 3.0 times that of the dry year (2.8 times for Xingzi River, 2.9 times for Xichuan River, and 3.0 times for Pingqiao River), demonstrating the dilution dominance mechanism. Xichuan River has the largest water pollution capacity, followed by Xingzi River, and the smallest is Pingqiao River. This is consistent with the order of basin area and runoff volume, reflecting that hydrological conditions are the primary factor controlling the water pollution capacity [15].

3.2 Annual Distribution Characteristics

The annual distribution of the river's pollutant absorption capacity is mainly controlled by the seasonal distribution of runoff [16]. Since all three rivers belong to typical rain-fed loess hilly gully areas, runoff is highly dependent on precipitation, and the annual distribution is extremely uneven: July to September is the flood season (accounting for 60% to 75% of the annual runoff), December to February is the low-water season (accounting for less than 5% of the annual runoff), and March to June and October to November are the transitional periods between normal flow and low flow.

3.2.1 Annual distribution characteristics of Xingzi River

The pollutant absorption capacity of Xingzi River shows a significant "single-peak" annual distribution, with the peak concentrated in July and August, and the trough in January and February (Figure 2). In a wet year, the COD pollutant absorption capacity reaches its maximum in August (171.87 t/a), and the minimum in January (5.03 t/a), with a range ratio of 34.2; the range ratios of ammonia nitrogen and TP are 34.0 and 34.4 respectively, indicating that the dilution and self-purification capacity is sharply enhanced in high-flow months. The combined COD pollutant absorption capacity of July and August is 343.49 t/a, accounting for 39.3% of the annual total; while the combined total of January to February and December is only 4.2% of the annual total. The distribution pattern in a normal flow year is similar to that in a wet year, but the range has decreased. The maximum COD pollutant absorption capacity occurs in July (61.89 t/a), and the minimum is in January (11.97 t/a), with a range ratio of 5.17. The pollutant absorption capacity in August (33.12 t/a) is slightly lower than that in July, reflecting that the flow in July (4.35 m^3/s) is higher than that in August (2.33 m^3/s), which is different from the wet year (the flow in August is the highest in the wet year). The range of the low-water year has further narrowed. The maximum COD pollutant absorption capacity occurs in August (40.38 t/a), and the minimum is in February (7.66 t/a), with a range ratio of 5.27. It is worth noting that the sum of the pollutant absorption capacity in the summer (July and August) in the low-water year (63.83 t/a) only accounts for 20.4% of the annual total, while in the wet year this proportion is as high as 39.3%, indicating that the dilution capacity in the summer of the low-water year is relatively weakened. If the concentrated input of non-point sources is superimposed during this period, the risk of water quality exceeding standards still exists in some local periods.

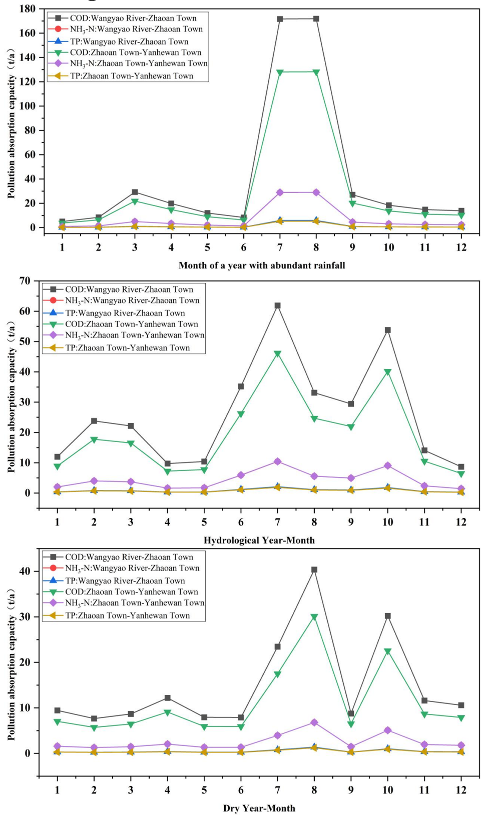

Figure 2. Pollution-Tolerant Capacity of the Xingzi River during Flood Years, Normal Years and Dry Years

3.2.2 Distribution characteristics of the Xichuan River within the year

The Xichuan River is the river with the largest drainage area and the highest runoff volume among the three rivers. Its pollutant absorption capacity also shows a single-peak distribution pattern within the year, but the variation range is significantly larger than that of the Xingzi River, and the differences between different river sections are more prominent (Figure 3). In the flood year, the COD absorption capacity reaches its peak in August (259.67 t/a at the entry - Zhuanyaowan section, approximately 497.2 t/a for the entire river section), and is the lowest in January (7.60 t/a at the entry - Zhuanyaowan section, approximately 17.46 t/a for the entire river section), with an extreme ratio of 28.5. The single-month absorption capacity in August accounts for 28.6% of the entire year (calculated based on the entry - Zhuanyaowan section), while the combined capacity of January-February and December is less than 5%. This extreme distribution characteristic within the year indicates that the Xichuan River is extremely sensitive to environmental loads during the dry season, and even a small increase in pollution may lead to water quality exceeding standards.

The distribution in the normal water year still maintains a single-peak pattern, but the peak month shifts to July (COD 92.38 t/a at the entry - Zhuanyaowan section), with 49.43 t/a in August. This is because the flow in July (2.37 m³/s) is higher than that in August (1.27 m³/s). The extreme ratio (July/January) is 5.17, which is highly consistent with the extreme ratio of the Xingzi River in the normal water year (5.17), reflecting that the two rivers have similar hydrological regulation capabilities in the normal water year. The peak occurs in August (58.78 t/a at the entry - Zhuanyaowan section), and the low point is in February (11.16 t/a), with an extreme ratio of 5.27. It is noteworthy that the absorption capacity in August of the Xichuan River during the dry season (58.78 t/a) is still higher than most months of the Xingzi River in the normal water year, indicating that its background absorption capacity is relatively strong.

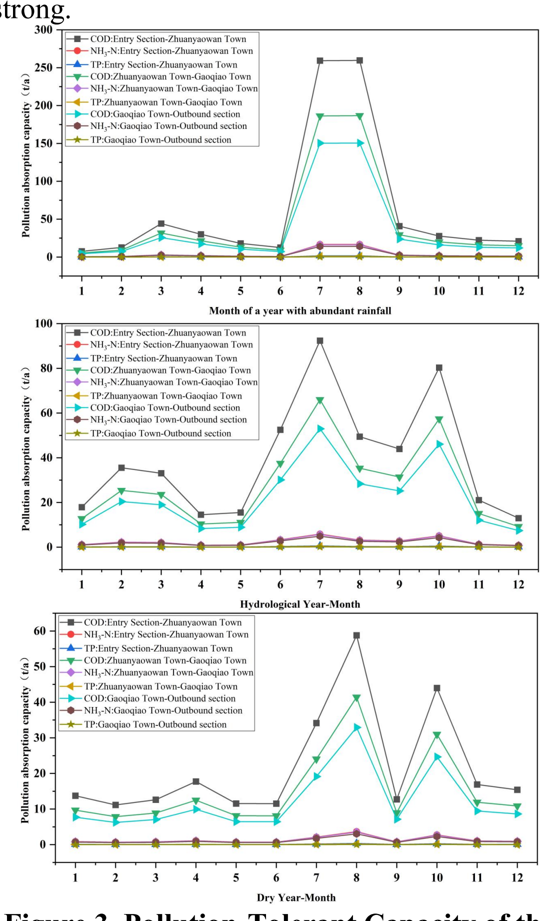

Figure 3. Pollution-Tolerant Capacity of the Xichuan River during Flood Years, Normal Years and Dry Years

3.2.3 Distribution characteristics of Pingqiao River within the year

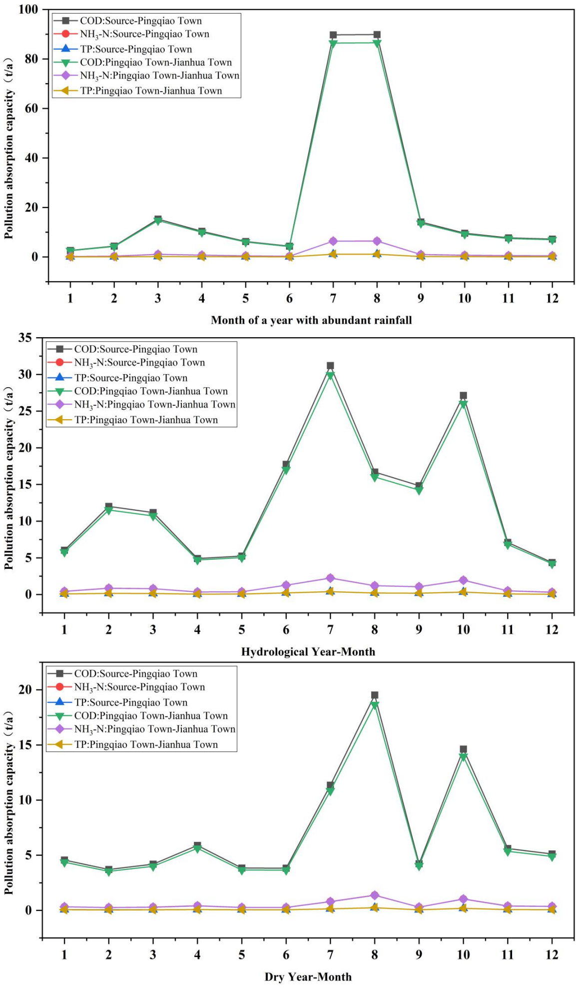

Figure 4. Pollutant Absorption Capacity of Pingqiao River in Flood Years, Normal Years and Dry Years

Pingqiao River is the river with the smallest drainage area and the lowest runoff volume among the three rivers. Its absolute capacity for pollutant absorption is the lowest, but the relative variation within the year is the greatest, exhibiting a very strong "pulsatile" characteristic (Figure 4). The COD absorption capacity in the flood year reaches its maximum in August (89.88 t/a from the source to Pingqiao section), and is the minimum in January (2.63 t/a), with an extreme value ratio of 34.2, similar to that of Xingzi River in the flood year. The single-month absorption capacity in August accounts for 34.3% of the annual total, while the combined capacity of January-February and December is only 3.8% of the annual total, and the absorption capacity during the dry season is almost negligible. This means that Pingqiao River has almost no self-purification capacity in winter, and any external input will directly lead to water quality deterioration. The peak value in the normal year occurs in July (31.21 t/a), and in August it is 16.70 t/a, with an extreme value ratio of (July/January) of 5.17. This is consistent with the extreme value ratio of Xingzi River and Xichuan River in the normal year (both 5.17), which is not a coincidence, but because all three rivers adopt the same annual flow type classification (based on the frequency curve of Wang Yao Reservoir), and the relative advantage of the July flow in the normal year. The peak value in the dry year occurs in August (19.53 t/a), the trough in February (3.71 t/a), and the extreme value ratio is 5.26. It is worth noting that the absorption capacity of Pingqiao River in August during the dry year (19.53 t/a) is even lower than that of Xingzi River in January of the normal year (11.97 t/a), indicating that even during the flood season, its absorption capacity is very limited.

3.3 Differences in Different River Sections

The pollution-carrying capacity of each month in the "Wang Yao Reservoir - Zhaoan Town" section of the Xingzi River is higher than that in the "Zhaoan Town - Yanhewan Town" section in the downstream. The difference is particularly significant in summer (COD in August at the upstream is 171.87 t/a, while at the downstream it is 128.23 t/a), and the downstream is approximately 74.6% of the upstream; the difference is relatively small in winter (5.03 t/a at the upstream vs 3.75 t/a at the downstream in January, a proportion of 74.5%). This is mainly due to the fact that the upstream receives the clear water discharged from Wang Yao Reservoir, with a lower background concentration, and there is less point-source pollution in the interval. The pollution-carrying capacity of Xichuan River shows a monotonically decreasing trend along the route. Taking August of the flood year as an example, the COD at the "Entry - Zhuanyaowan" section is 259.67 t/a, at the "Zhuanyaowan- Gaoqiao" section it is 186.66 t/a (approximately 71.9% of the upstream), and at the "Gaoqiao - Exit" section it is 150.52 t/a (approximately 58.0% of the upstream). The reduction range is much larger than that of Xingzi River, mainly because the towns (Zhuanyaowan, Gaoqiao) in the middle and lower reaches of Xichuan River have a dense population, and rural domestic sewage inflows cause the background concentration to increase along the route, thereby compressing the pollution-carrying space for the downstream. The difference in pollution-carrying capacity between the "Source - Pingqiao Town" section and the "Pingqiao Town - Jianhua Town" section in the upstream and downstream of Pingqiao River is very small. Taking August of the flood year as an example, the upstream is 89.88 t/a, and the downstream is 86.54 t/a, with the downstream being only 3.7% lower than the upstream; the difference in August of the dry year is also less than 5%. This reflects that the pollution input along the route of Pingqiao River is relatively uniform, and there is no sudden change in concentration caused by large reservoirs or concentrated sewage discharge from towns.

4. Discussion

4.1 Quantitative Relationship between Pollution-Carrying Capacity and Design Flow

A regression analysis was conducted on the pollution-carrying capacity (M) of each month and the corresponding design flow (Q) (n = 36, covering 3 rivers×12 months), and the following relationship was obtained:

COD: $M=128.4Q+2.35$, $R^2=0.91$

NH_3-N: $M=18.7Q+0.42$, $R^2=0.88$

TP: $M=3.96Q-0.13$, $R^2=0.86$

It indicates that the pollutant absorption capacity is highly linearly correlated with the runoff volume. For every 1 m^3/s increase in flow rate, the average COD absorption capacity increases by approximately 128 t/a. This relationship can be used to quickly estimate the absorption capacity under different flow scenarios and has practical value for water resource scheduling and pollution emergency control.

4.2 Uncertainty of Parameters and Computational Robustness

Although this study determined the parameters based on procedures and measured data, there is still uncertainty: (1) The K value is greatly affected by water temperature. In this calculation, the corresponding value of the annual average water temperature was used, and the decrease in K value during winter (possibly by 30% to 50%) was not considered. Therefore, the actual absorption capacity during the dry season may be smaller than the calculated value; (2) the non-point source inflow coefficient was taken as a fixed value of 0.02, and the distinction between storm and base flow conditions was not made. Under extreme rainfall events, the load from sources may increase by 2 to 5 times (Jin et al., 2022). It is recommended to conduct synchronous hydrological-water quality monitoring in different seasons, establish a dynamic K value function, and optimize the estimation of surface sources using SWAT and other semi-distributed models.

4.3 Insights for Water Environmental Management

Selection of Total Control Baseline: Since the absorption capacity during the dry season is much lower than the annual average, if the annual total is used as the baseline, it may mask the over-limit risk during the dry season [17]. It is recommended to use the monthly absorption capacity corresponding to the 90% guarantee rate of the minimum flow in the driest month as the upper limit for each month's pollutant discharge control. Prioritize pollution sources: According to Table 2-3, rural domestic sewage is the main contributor of COD and ammonia nitrogen, and livestock and poultry breeding is the main control source of TP. Rural small-scale sewage treatment facilities (such as artificial wetlands, integrated A^2O) should be prioritized for construction, and the utilization of livestock manure resources (composting, biogas) should be promoted to reduce direct discharge. Optimization of water quality monitoring: The current monitoring is once every quarter, which is difficult to capture the short-term deterioration during the dry season. It is recommended to increase monitoring frequency to once a month in winter (December - February) and set up automatic monitoring micro-stations at the 8 main tributary confluence entrances.

4.4 Research Limitations and Prospects

This study still has the following limitations: (1) The one-dimensional model was used, and the regulation effect of the reservoir (Wang Yao Reservoir) on downstream flow was not considered; (2) The adsorption-release process of pollutants in the sediment was not simulated, which may underestimate the endogenous load of phosphorus; (3) Only COD, ammonia nitrogen, and TP were calculated, and no heavy metals or emerging pollutants were involved. Future studies can be conducted using MIKE11 or EFDC models for two-dimensional/three-dimensional simulations and incorporate the prediction of the impact of climate change on runoff and K value.

5. Conclusion

Under the 90% guarantee rate hydrological conditions, the COD, ammonia nitrogen, and TP absorption capacities of Xingzi River, Xichuan River, and Pingqiao River in flood years, normal years, and dry years are all positive. The current pollution load does not exceed the absorption capacity during the dry year. The water quality of all three rivers can meet the Class III standard, and there is a certain safety margin. The absorption capacity shows significant spatiotemporal differentiation: temporally, flood years > normal years > dry years; in summer (July - August), the absorption capacity is 4 to 34 times that of winter (January - February); spatially, Xichuan River has the largest value (COD reaches 1737.48 t/a), followed by Xingzi River, and Pingqiao River is the smallest, and the upstream sections are generally higher than the downstream sections. The absorption capacity is highly significantly positively correlated with the runoff volume ($R^2 > 0.85$), and the comprehensive attenuation coefficient (K value) is the most sensitive parameter for the calculation results (a disturbance of ±20% causes a result change of ±18% to ±22%).

This study has the following deficiencies: the one-dimensional water quality model did not consider lateral and vertical mixing, which may overestimate the absorption capacity in local mixing zones; the K value was taken as the annual average, which did not reflect the impact of a 30% to 50% decrease in low temperatures during winter, resulting in optimistic results during the dry season; the non-point source load was estimated based on statistical yearbooks and fixed inflow coefficient, without distinguishing between storm runoff and base flow conditions, nor considering the temporal heterogeneity of land use and slope. The scheduling rules of Wangyao Reservoir were not coupled, resulting in deviations in the calculation of the downstream river section; only three conventional indicators (COD, ammonia nitrogen, and TP) were calculated, without covering heavy metals and emerging pollutants. In the future, seasonal synchronous hydrological-water quality monitoring should be carried out, and a dynamic function of the K value changing with water temperature and flow rate should be established; distributed models such as SWAT should be introduced to achieve the dynamic estimation of non-point source loads in time and space; the reservoir scheduling module should be embedded to simulate different operation scenarios; heavy metals, pesticides, and emerging pollutants should be gradually included in the calculation framework; the pollutant discharge capacity in the dry season should be used as the worst-case benchmark for total pollution control, with particular emphasis on rural domestic sewage (COD, ammonia nitrogen) and livestock and poultry breeding (TP); the frequency of water quality monitoring should be increased in winter, and a regional dynamic K value database should be constructed to provide support for refined water environment management.

References

[1] Ke Z. Study on the dynamic prediction and optimum regulation scheme of water resource carrying capacity in the yellow river basin. Scientific Reports, 2025, 15: 8188.

[2] Mohsen Dehghani D, Britta S. River quality management: Integrating uncertainty, failure probability, and assimilation capacity. Ecological Informatics, 2024, 83: 102829.

[3] He S, Yutong Z, et al. Spatiotemporal characteristics, drivers, sources, and health risks of nitrate and sulfate in groundwater on the Chinese Loess Plateau. Water Research, 2026, 288: 124531.

[4] Zijun L, Qingchun Y, et al. Spatiotemporal variability of groundwater chemistry, source identification and health risks in the southern Chinese Loess Plateau. Ecotoxicology and Environmental Safety, 2025, 289: 117429.

[5] Fang P, Ma Y, Shen J, et al. Problems and countermeasures of water ecological environment in Yanhe River Basin. People's Yellow River, 2022, 44(01): 80-82+88.

[6] Zhang Y L. Development of the basic concept of water environmental capacity. Research of Environmental Sciences, 1992(03): 59-61.

[7] iu H D. Study on water environmental capacity of typical polluted reaches of Yanhe River. Xi'an: Northwest University, 2021.

[8] Zhang Q H, Tan F F, Wu Z H, et al. Calculation of water environmental capacity of ammonia nitrogen and total phosphorus in Laodao River Basin of the Xiangjiang

River. Journal of Environmental Engineering Technology, 2022, 12(2): 468-476.
[9] Lao G M. Sensitivity analysis of parameters in one-dimensional model for calculating water environmental capacity. Zhejiang Hydrotechnics, 2003(02): 18-19.
[10]Zhou R, Wang B, Lin H D, et al. Application of one-dimensional water quality model combined with improved export coefficient method in estimation of non-point source pollution load in watershed. Journal of Jilin University, 2021, 51(2): 505-515.
[11]Bo P, Kun L. An Analytical Approach for Initial Allocation of Discharge Permits with Consideration of the Water Environmental Capacity and Industrial Technical Feasibility. Sustainability, 2021, 13(24): 13743.
[12]Wang X D. Study on water environmental capacity calculation and pollution prevention and control of Weihe River in Shaanxi Province based on process. Xi'an: Chang'an University, 2022.
[13]Jin H, Chen W, Zhao Z, et al. New Framework for Dynamic Water Environmental Capacity Estimation Integrating the Hydro-Environmental Model and Load–Duration Curve Method—A Case Study in Data-Scarce Luanhe River Basin. International Journal of Environmental Research and Public Health, 2022, 19(14):8389.
[14]Zhang Q, Tan F, Wu Z, et al., Calculation of water environmental capacity of ammonia-nitrogen and total phosphorus in Laodao River Basin of the Xiang River. Journal of Environmental Engineering Technology, 2022, 12(2): 468-476.
[15]Obin N, Tao H, et al. Research on Water Quality Simulation and Water Environmental Capacity in Lushui River Based on WASP Model. Water, 2021, 13(20): 2819.
[16]Song Y, & Wang H. Study on the Stage Method of the Water Environmental Capacity Flood Season in the Ningxia Section of the Yellow River. Hydrology, 2025, 12(1): 10.
[17]Wang J, Tian C. Study of the allocation strategy of water pollutant emission permits under a bidirectional ecological compensation mechanism: A case study of China's Yellow River Basin. Journal of Cleaner Production / ResearchGate, Art. 2024, 141258.